ISSN 0016-7932, Geomagnetism and Aeronomy, 2019, Vol. 59, No. 8, pp. 971–979. © Pleiades Publishing, Ltd., 2019.

Spatio-Temporal Prediction of Ionospheric Total Electron Content Using an Adaptive Data Fusion Technique

Faruk Erken[a], *, Secil Karatay[a], **, and Ali Cinar[a], ***

[a]*Department of Electrical and Electronics Engineering, Kastamonu University, Kastamonu, Turkey*

**e-mail: ferken@kastamonu.edu.tr*

***e-mail: skaratay@kastamonu.edu.tr*

****e-mail: acinar@kastamonu.edu.tr*

Received June 21, 2018; revised April 1, 2019; accepted April 25, 2019

Abstract—The ionosphere, a part of upper atmosphere, plays an important role on the propagation of radio waves. Hence, understanding, remote sensing and monitoring of the ionospheric phenomena can provide a compressive description to the physical process that are affected by the behavior of ionosphere. One of descriptive quantity of ionosphere is Total Electron Content (TEC). TEC is the total number of electrons integrated between two points and characterized by observing carrier phase delays of received radio signals transmitted from satellites located above the ionosphere, often using Global Positioning System (GPS) satellites. In this study, TEC is predicted from TEC estimates obtained from GPS network located in Turkey in space and time using an Adaptive Data Fusion Technique (ADF). It is observed that characteristic distributions of the predict TEC and original TEC values are similar with each other. Mean Square Errors are less than 4 TECU. ADF has a high performance for the spatio-temporal prediction when the results are compared with the techniques used in the related studies in the literature.

DOI: 10.1134/S001679321908005X

1. INTRODUCTION

Ionosphere in an interaction layer between the earth's neutral atmosphere and the sun which lies between 50 and 1000 km altitudes of atmosphere. The ionosphere is significantly ionized by solar radiation and free electrons in the ionosphere have a unique importance in the radio communication. The radio waves reach the larger distances by reflecting from the ionosphere. Also, the ionosphere is significant error source for satellite based communication, positioning and navigation systems and detrimental effects on the amplitude and phases of received signals. However, these errors can be reduced by some models in order to study the temporal and spatial variations of the ionosphere. The performance of the communication systems can provide the predicting of the ionospheric parameters and variability. Empirical models of the ionosphere are widely used to organize radio communication and to solve the direction finding and radio location problems. Troitsky et al. (2007) demonstrated that these models depend on the trajectory calculations and make it possible to easily calculate necessary signal characteristics.

Solar, geomagnetic and gravitational activities cause some anomalies which have some effects on space based communication, navigation and positioning systems. Afraimovich et al. (2013) proposed a technique that can be used to analyze the state of near-Earth space interaction and the spectrum and composition of the ionospheric disturbances caused by solar eclipses, solar flares and geomagnetic storms and they show that the ionosphere displays significant changes during the geomagnetic storms and Solar Flares (SFs). As a result of a magnetic storm, large-scale Total Electron Content disturbances occur almost simultaneously in the ionosphere both in the Northern and Southern Hemispheres. Karatay et al. (2017) shows that there is a positive linear relation between the Sunspot Number (SSN) and TEC. Increase in solar activity results in increase in spread and metric distances between different regions at mid-latitudes and different years of solar maximum (especially during winter solstice and autumn equinox). As given in studies such as Calais and Minster (1995), Pulinets et al. (2006), it has been observed that seismic activity can cause deviations in the ionospheric plasma that can be detected as disturbances. As given in Polekh et al. (2006), ionospheric disturbances show a complicated complex of events depending on many factors such as parameters of the interplanetary magnetic field, intensity of the geomagnetic storm, coordinates and local time of the observation point. These disturbances can be categorized with respect to their amplitude, duration and frequency. Ionospheric researches have greatly utilized from the space program with the related development

of instruments for ballons, rockets and satellites. The combination of remote sensing and direct measurements are important for characterizing the ionosphere and communication, navigation and positioning systems as discussed in Kelly (2009).

The ionospheric irregularities are described mainly by the electron density distribution that can characterize the variations and disturbances of ionosphere. Radio propagation in magnetized plasma depends on electron density and magnetic field along propagation path. One of the most important ionospheric parameter, which is a function of the electron density, is Total Electron Content (TEC). TEC, which is defined as the line integral of electron density on a given ray path, is an observable parameter that can be estimated from ground based Global Navigation Satellite System (GNSS) receivers. The unit of TEC is TECU that is 10^{16} electrons per square meter described in Hofmann et al. (1992) and several papers (McNamara, 1994; Kouris et al., 2005; Kim and Tinin, 2007). Global Positioning System (GPS) is the prominent system that is used in estimation of TEC. The observing carrier phase delays of received signals transmitted from GPS satellites located above the ionosphere are used in the estimating GPS-TEC. Kim and Tinin (2007) presented that the error of range determination introduced by the ionosphere reaches 20–30 m under quiet conditions and considerably increases during geomagnetic storms. In the dual frequency method, the phase and (or) group paths of a GPS signal are measured at two frequencies. Using the known dependence of these characteristics on frequency, one subsequently finds two quantities: range and Total Electron Content along a line of sight of a GPS receiver and a GPS transmitter. In GPS-TEC computation it is defined that the Slant TEC (STEC) is the linear integral of the electron density along any satellite-receiver ray path as given in studies such as Arikan et al. (2004), Arikan et al. (2008), Nayir et al. (2007) and Brunini and Azpilicueta (2010). GPS observations can provide very precise estimation of the STEC. The TEC in the local zenith direction at the ionospheric pierce point is known as Vertical TEC (VTEC). STEC is converted to VTEC using a mapping function that is discussed in detail by Arikan et al. (2003), Arikan et al. (2004), Arikan et al. (2008) and Nayir et al. (2007). There are techniques based on different free-to-use software in the literature as given in studies such as Arikan et al. (2003), Yasyukevich (2015), Seemala (2017) that are used for TEC estimation. In this paper, the VTEC data with 2.5 min time resolution is computed using IONOLAB-TEC technique. IONOLAB-TEC is state-of-the-art signal processing technique for GPS-TEC estimation for a single station. IONOLAB-TEC provides accurate, reliable and robust GPS-TEC estimation with some limit for any high latitude, midlatitude, or equatorial GPS station (www.ionolab.org). Current version of IONOLAB-TEC, which can be used online or can be downloaded from www.ionolab.org site as *.exe format, can estimate GPS-TEC in the temporal resolution of any RINEX file. IONOLAB-TEC can be estimated in enough accuracy with 30 s and 2.5 min.

Total Electron Content also shows significant variations in both space and time depending on solar and geomagnetic conditions discussed in detail by Rishbeth and Garriott (1969) and Kelly (2009), geographic location and seasons as discussed in Karatay et al (2017) and strong seismic activity given in detail by Liu et al. (2004), Liperovsky et al. (2008) and Karatay et al. (2010). Astafyeva and Heki (2011) showed that even under solar minimum, the main driver for the ionospheric disturbance is the geomagnetic activity. Space weather effects mostly produce significant changes in TEC distributions, even during solar minimum. Perevalova et al. (2010) demonstrated that the atmospheric winds significantly affect to the day-to-day variability of TEC. Abnormal diurnal variations in TEC distributions (evening maximum, near-noon minimum) are observed at mid and high latitudes under the influence of the atmospheric wind. These conditions have negative effects also on the navigation systems. GPS signals are affected by multipath, environmental or physical conditions and various disruptions of data or problems like cycle slips that may occur in the estimation of TEC. At the same time, the receiver hardware can cause TEC to be computed in discrete epochs. State-of-art receiver can measure signals with 100 Hz cadence, which is more than enough for studying ionospheric processes. There are many alternative models that are developed in literature for providing the lack of data due to the discrete epochs and the exact data such as Mannucci et al. (1998), Iijima et al. (1999), Teunissen and Odijk (2003), Arikan et al. (2011) Deviren et al. (2013) and Tuna et al. (2015).

Forecasting and nowcasting of TEC are important in the planning and operation of Earth-space and satellite-to-satellite communication systems. Therefore, several papers are devoted to predicting of TEC in space and time. One of the parameter estimation method, namely Adaptive Data Fusion (ADF), is close in the nature to the Random Forest technique that is used for temporal prediction of TEC by Zhukov et al. (2018). Adaptive Data Fusion (ADF) is described as a multilevel, multifaceted process that is dealing with the automatic detection, association, correlation, estimation, and combination of data and information from single and multiple sources which is divided into four steps, namely object refinement, situation assessment, threat assessment and process refinement (Klein, 1993). In this study, an ADF algorithm is developed for prediction of TEC, which is based on IONOLAB-TEC software, combined with weights updated band on the gradient of the error. TEC data used in this study is obtained from Turkish National Permanent GPS Network (TNPGN-Active) stations during May and October of 2010 and May and October of 2011. ADF is used for the first time in the literature in this context. Results are made separately in time and space. The Adaptive

Data Fusion (ADF) Technique used in the study and the results are presented in Sections 2 and 3, respectively.

2. ADAPTIVE DATA FUSION TECHNIQUE

Adaptive Data Fusion (ADF) is a linear combining algorithm for subdata that is developed for many applications. For example, Benaskeur and Rheaume (2007) showed that ADF can be used in distributed military surveillance operations, at both the tactical and operational levels. A more robust algorithm for data fusion in presence of all uncertainties is needed in this technique. Wu et al. (2014) investigated three adaptive methods and showed that data fusion is an effective approach because of the large number of competitive techniques. As reported in Linas and Singh (1998) and Hong (1991), by reducing uncertainty in the existing pieces of information and providing means to conclude about the missing pieces, data fusion processing supports the decision-makers in compiling and analyzing.

In the literature such as Gunay et al. (2012), Erken et al. (2016), and Karaman et al. (2018), an online learning structure is used for various image analysis and computer vision applications. Data are linearly combined with weights according to an active fusion method based on performing orthogonal projections onto convex sets describing these values. The predicted data are obtained by weighting and combining from other data which are correlated with the missing data. The error term is acquired with the gradient of the difference between each predicted and available data. The weighted values in data are regenerated according to the contribution of an increase or a decrease in the error term. Initially, the weights are accepted as equal and then they are regenerated using ADF algorithm.

Let $\mathbf{y}_u(d)$ represent the set of VTEC data of length N at time step n estimated for day d of any receiver u as:

$$\mathbf{y}_u(d) = \left[y_u(1,d) \ldots\ldots\ldots y_u(n,d) \ldots\ldots\ldots y_u(N,d)\right]^T, \quad (1)$$

where T is the transpose operator. M is the window size that can be defined as the number of the previous days used for the temporal prediction of a day d. In order to predict the value at any time step, n values of vectors $\mathbf{y}_u(d)$ for the window size M are obtained as follow:

$$\mathbf{y}_u(n,d) = \left[y_u(n,1) \ldots\ldots\ldots y_u(n,d) \ldots\ldots\ldots y_u(n,M)\right]^T. \quad (2)$$

The current weight vector can be defined as (Erken et al., 2016):

$$\mathbf{w}_u(n,d) = \left[w_u(n,1) \ldots\ldots w_u(n,d) \ldots\ldots w_u(n,M)\right]^T. \quad (3)$$

Using Equation 3, the estimate of compound value $\hat{y}_u(n,d)$ of any sample at any time step is defined as follow (Erken et al., 2016):

$$\hat{y}_u(n,d) = \mathbf{y}_\mathbf{u}^T(d)\,\mathbf{w}_u(d) = \sum_{n=1}^{M} w_u(n,d)\,y_u(n,d). \quad (4)$$

The error $e_u(n,d)$ and the minimizing mean square error of regenerated weights can be defined as follows, respectively (Erken et al., 2016):

$$e_u(n,d) = y_u(n,d) - \hat{y}_u(n,d), \quad (5)$$

$$\min_{w_u} E\left[\left(y_u(n,d) - \hat{y}_u(n,d)\right)^2\right], \quad i = 1, \ldots\ldots M, \quad (6)$$

where E is the expectation operator. In order to obtain minimum value of E, Equation (6) is derivatived with respect to weights and equal to zero (Erken et al., 2016):

$$\frac{\partial E}{\partial w} = -2E\left[\left(y_u(n,d) - \hat{y}_u(n,d)\right) y_u(n,d)\right] = -2E\left[\left(e(n,d)\,y(n,d)\right)\right] = 0, \quad i = 1, \ldots\ldots M. \quad (7)$$

Thus, a set of M equations are obtained, namely Weiner Solution. The gradient in Equation (7) can be used in steepest descent algorithm in order to obtain an iterative solution to the minimisation problem in Equation (6) as follow (Erken et al., 2016):

$$w_u(n+1,d) = w_u(n,d) + \lambda E\left[\left(e(n,d)\,y_u(n,d)\right)\right]. \quad (8)$$

In the above equation, the step size can be replaced by (Erken et al., 2016):

$$\frac{\mu}{\left\|y_u(n,d)\right\|^2}, \quad (9)$$

where μ is the update parameter. Then Equation (8) can be re-written as in Normalized Least Mean Square Algorithm (N-LMS) as defined earlier by Haykin and Widrow (2003) as follow:

$$w_u(n+1,d) = w_u(n,d) + \mu\frac{e_u(n,d)}{\left\|y_u(n,d)\right\|^2}\,y_u(n,d). \quad (10)$$

This algoritm provides the controlled feedback mechanism based on the error term. Weights of the data are adaptively regenareted according to Equation (10).

In order to measure the errors or deviations between the predicted and real values, Mean Square Error (MSE) is obtained as follow (Erturk et al., 2008):

$$MSE_u(d) = \sqrt{\frac{1}{N}\sum_{n=1}^{N}\left(\hat{y}_u(n,d) - y_u(n,d)\right)^2}. \quad (11)$$

Where $\hat{y}_u(n,d)$ denotes the predicted the VTEC obtained from ADF algoritm and $y_u(n,d)$ denotes the

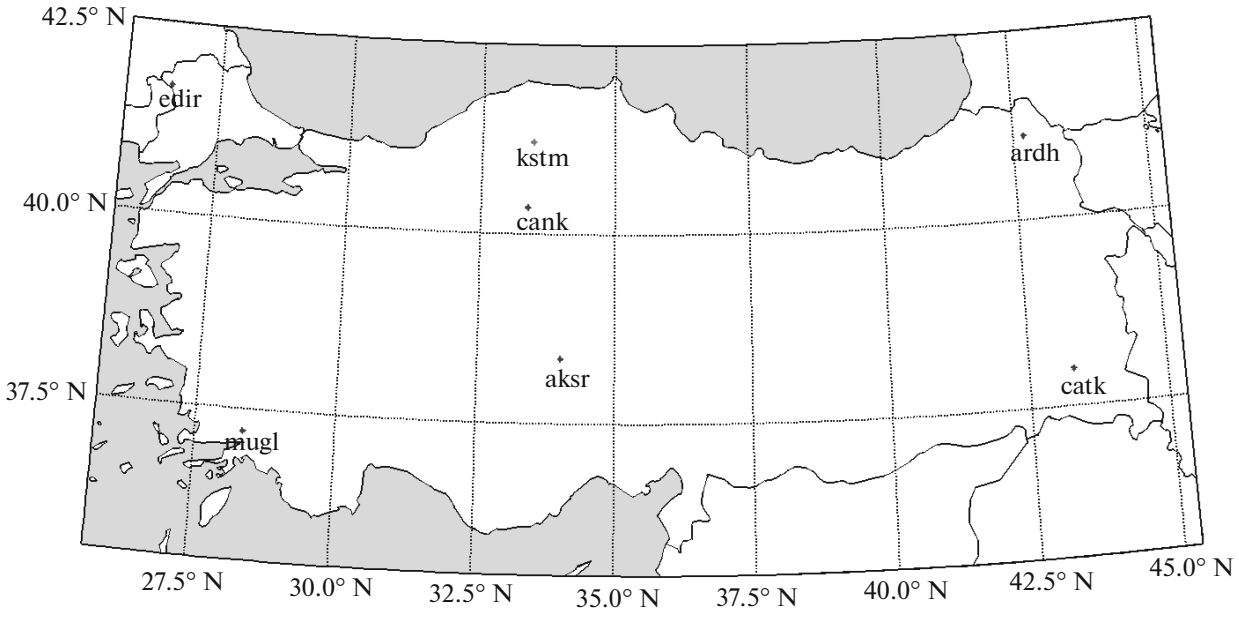

Fig. 1. TNPGN-Active GPS stations located in Turkey in a 2.5° by 2.5° resolution in latitude and longitude, respectively. The station with red star is chosen for the predicted station and the stations with blue stars are used for the prediction.

VTEC from GPS mesaurements for receiver u and day d. N is the total number of samples in a day. For the prediction in space, $\hat{\mathbf{y}}_d(n,u)$, $\mathbf{w}_d(n,u)$ and $MSE_d(n,u)$ are computed for any u station, respectively.

3. RESULTS AND DISCUSSION

The technique described in Section 2 is applied to TEC data to predict the Vertical Total Electron Content (VTEC) in space and time. The raw data for corresponding GPS stations in the region of the interest are obtained from Turkish National Permanent GPS Network (TNPGN-Active) during May and October of 2010 and 2011. The geographical locations of representative stations are shown in Fig. 1 and Table 1 in alphabetical order. The VTEC values for each station are estimated using IONOLAB-TEC technique, a high resolution, reliable and accurate GPS-TEC estimation algorithm developed by IONOLAB group as defined in detail by Arikan et al. (2003), Arikan et al. (2007), Nayir et al. (2007), Sezen et al. (2013) and currently available at www.ionolab.org.. The prediction is obtained separately in time and space.

Table 1. Locations of the selected TNPGN-Active receivers

Station	Station Code	Latitude, °N	Longitude, °E
Aksaray	aksr	38.22	33.59
Ardahan	ardh	41.06	42.41
Çankiri	cank	40.36	33.36
Catak	catk	38.00	43.03
Edirne	edir	41.40	26.33
Kastamonu	kstm	41.22	33.46
Mugla	mugl	37.12	28.21

In Figure 2, a block diagram is given for the temporal prediction. $y_u(n,d)$ in the block diagram represents the VTEC values belonging to the same time in previous days for the time to be estimated. Estimated VTEC values of this time is obtained by weighting with ADF technique. M is the window size and it indicates that the prediction method will use the VTEC value for the number of days before the estimated day. Initially, the weights are accepted as equal to $1/M$. The weights are updated according to the contribution of an increase or decrease in the error term. The error term $e_u(n,d)$ is obtained with the difference between the intrinsic value and the predicted value at any time. Then, they are updated using the ADF algorithm during the test. Since weight values are initially considered equal and constantly updated for every new day to be estimated, the prediction starts a few days before. In the spatial prediction, VTEC values of the desired station are predicted from VTEC values of the stations to be used in the prediction for each time to be estimated by weighting with ADF technique. Here, the window size M is the number of the stations that will be used in the prediction. The weight values obtained from recent days using VTEC values are used to predict the VTEC values of the station that will be predicted.

In the temporal prediction, VTEC values of kstm is predicted using Equation 4. There are two chosen periods between May 08 and 17, 2011 and October 16

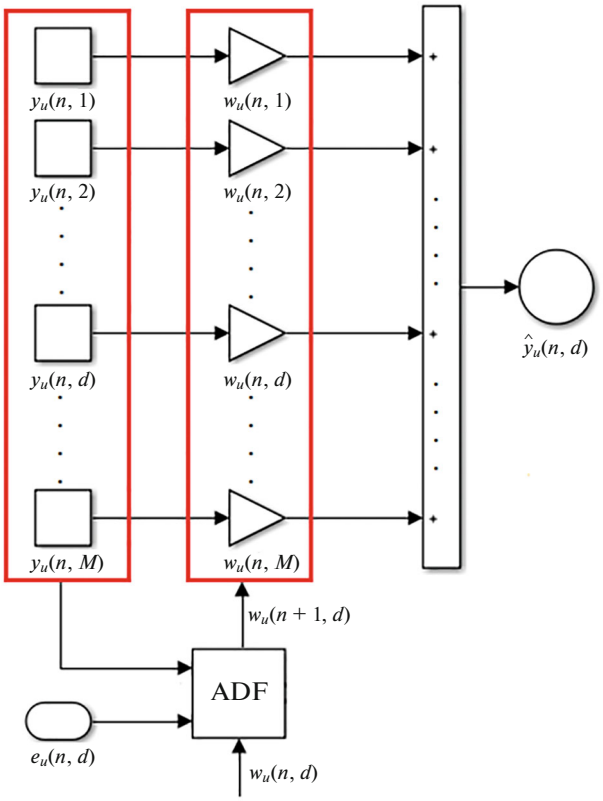

Fig. 2. Block diagram for temporal prediction.

and 25, 2011. Window size is the size of the vector that contains the previous 10 days data used for the prediction. This vector includes data of the same time before the predicted day. The updating parameter μ is chosen 0.5 where the error $e_u(n,d)$ has the smallest value. First, the algorithm accepts that the weights are equal and updated according to the error term. The first 10 days starting from 20 days before the day to be predicted are used for the training and the last 10 days are used for the prediction. Since the weights should reach the appropriate value, the first 10 days in this study are accepted for educational purposes and not taken into consideration. It is observed that the predictions in this period are close to intrinsic values. Mean Square Errors (MSE) vary between 2 and 3.5. As an example to this result, in Figs. 3 and 4, the distributions of predicted values and real TEC for kstm are given for May 8–17, 2011 and October 16–25, 2011, respectively. 2011 can be accepted as solar maximum year. Sun Spot Numbers (SSNs) are 41.6 and 88.0 on May and October, respectively (https://www.ngdc.noaa.gov/stp/space-weather/solar-data/solar-indices/sunspot-numbers). Kp and Ap indices reach up to 5 and 16 on April 20; 5 and 24 on April 30; 5 and 20 on May 2 (ftp://ftp.swpc.noaa.gov/pub/indices/old_indices/). Maximum observed MSE value on May 10 shown with an arrow in the figure and greater difference between the predicted TEC and the real TEC in Fig. 3 can be due to the previous geomagnetically disturbed days.

Figure 4 shows the 10-days distributions of the temporal-predicted TEC and real TEC between October 16 and 25, 2011. Kp and Ap indices reach up to 8 and 67 on September 26; 7 and 30 on September 27; 7 and 23 on October 24; 6 and 25 on October 25, respectively (https://www.ngdc.noaa.gov/stp/space-weather/solar-data/solar-indices/sunspot-numbers). These differences observed on October 21 and 25 that are demonstrated with arrows in Fig. 4, can also be due to the intense geomagnetic activity. Maximum MSE is observed on October 25 in this period. The other predicted values are close to real TEC estimates both in May and October periods. Thus, the ADF can be accepted as the susceptible tool for seeing the geomagnetic disturbance. According to the MSE values calcu-

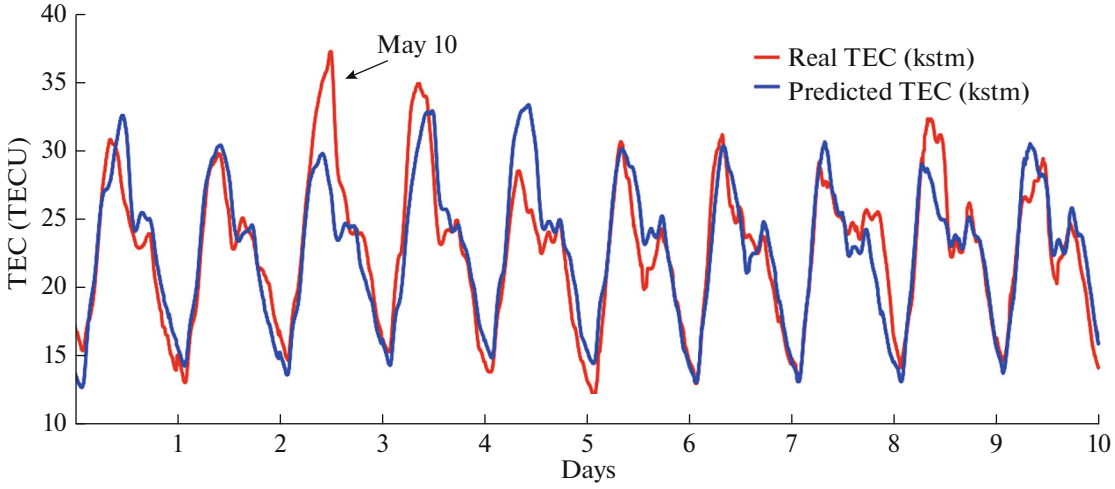

Fig. 3. 10-days distributions of the temporal-predicted TEC and real TEC between May 08 and 17, 2011.

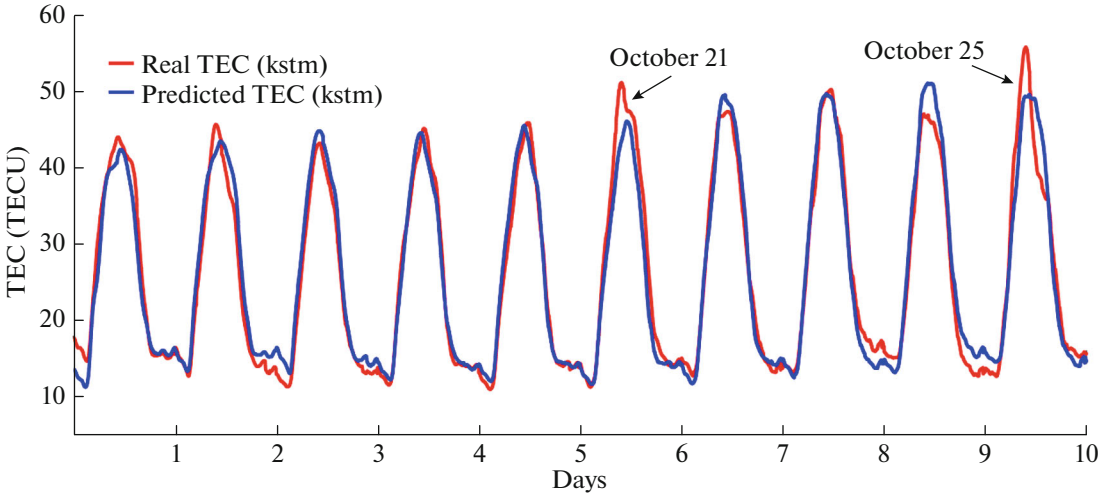

Fig. 4. 10-days distributions of the temporal-predicted TEC and real TEC between October 16 and 25, 2011.

lated for prediction in time, ADF can be successful tool to use for the temporal prediction.

In the spatial prediction, TEC values for kstm is predicted using data from 6 TNPGN-Active stations given in Fig. 1 for 10 days for two periods between May 2 and 11 and October 2 and 11, 2010, respectively. The window size equals to the number of the chosen stations in this group of the application. So the window size M and the updating parameter μ are chosen as 6 and 0.5, respectively. Initially, one-day TEC estimates for the central station kstm before 10 days used for the spatio-prediction are inputted to the algorithm for the training. First value $y_d(n,u)$ of TEC data is weighted by $1/M$. For the next n, the ADF algorithm and TEC estimates of kstm are multiplied by the weights. The weights are continuously updated depending on $e_d(n,u)$ obtained by the comparison of the $\hat{y}_d(n,u)$ with $y_d(n,u)$. Thus, the weights computed for all n of a day are used for the spatio-prediction of the following 10 days. In order to verify the results, TEC estimates from one of the receivers given in Fig. 1 is chosen as central station to control the predicted TEC. The spatio-prediction is based on the remaining six stations. TEC data predicted from the ADF algorithm using six stations are compared with the original TEC estimates for the central station with using Equation (11). This validation is also checked for the temporal prediction. TEC predictions are compared with the actual 10-days TEC estimates for the central station using Equation (11).

In the spatial prediction, it is observed that the predicted TEC has very close values to TEC although MSEs in spatio-prediction are greater than those in the temporal-prediction. SSNs are 8.7 and 23.5 on May and October 2010, respectively (https://www.ngdc.noaa.gov/stp/space-weather/solar-data/solar-indices/sunspot-numbers). 2010 is a solar minimum. Maximum values of Kp and Ap indices are 4 and 13 on May and 4 and 14 on October, respectively (ftp://ftp.swpc.noaa.gov/pub/indices/old_indices/). There is no too much difference observed between the predicted TEC and the real TEC. In Figs. 5 and 6, distributions of the predicted TEC obtained using data from six stations located at corner regions and middle zone of Turkey and real TEC are presented for May 2–11 and October 2–11, 2010, respectively. It is observed from two figures, the predicted TEC and the real TEC match with each other. Characteristics of the distribution of real TEC values occur in the predicted values. So the ADF algorithm can be used for the spatio-prediction.

Table 2 shows the Mean Square Errors (MSEs) both for spatio and temporal predictions. Both for spatio and temporal predictions, MSEs are less than 4 TECU. Cander (2003) focused on the mapping and forecasting of the ionospheric space weather conditions in near-real-time over Europe. The prediction error in this study is less than 4 TECU. Habarulema et al. (2011) analyzed this problem based on neural networks. They demonstrated that temporal extrapolation is better during quiet periods than magnetic storm periods. Zhukov et al. (2018) used the Random Forest technique for the temporal prediction of TEC. In this paper, the error is obtained 2 TECU for machine learning based models and 4 TECU for linear regression model. In Tulunay et al. (2004), the prediction of TEC is performed with neural network based models. Absolute error is less than 7 TECU and cross correlation coefficients are greater than 0.8. In Garcia-Rigo et al. (2011), VTEC is predicted using Discrete Cosine Transform (DCT), which is widely used in image compression. The errors in the related study vary between 2 TECU and 4.56 TECU.

When the Mean Square Error values provided in Table 2 are compared with the results of the studies mentioned above, it is observed that ADF algorithm is

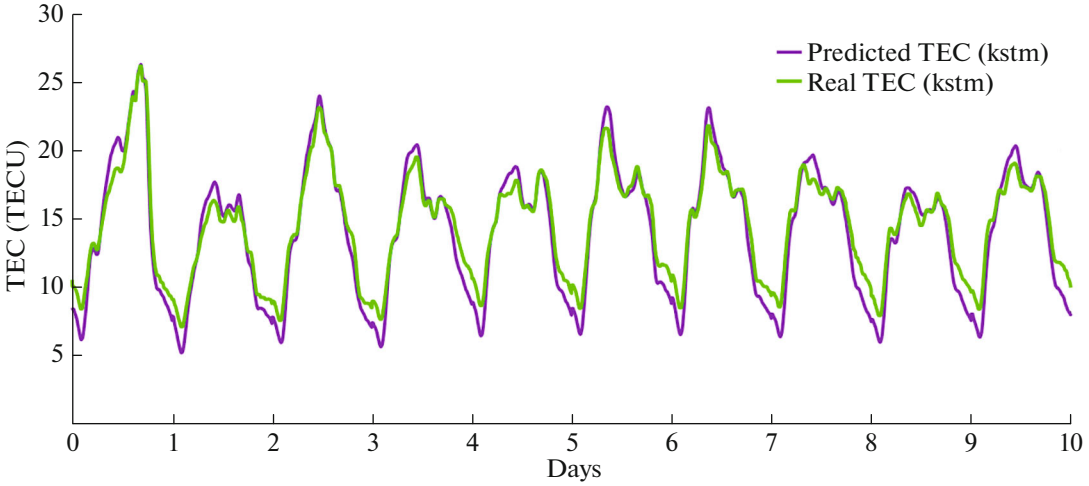

Fig. 5. 10-days distributions of spatio-predicted TEC and real TEC between May 02 and 11, 2010.

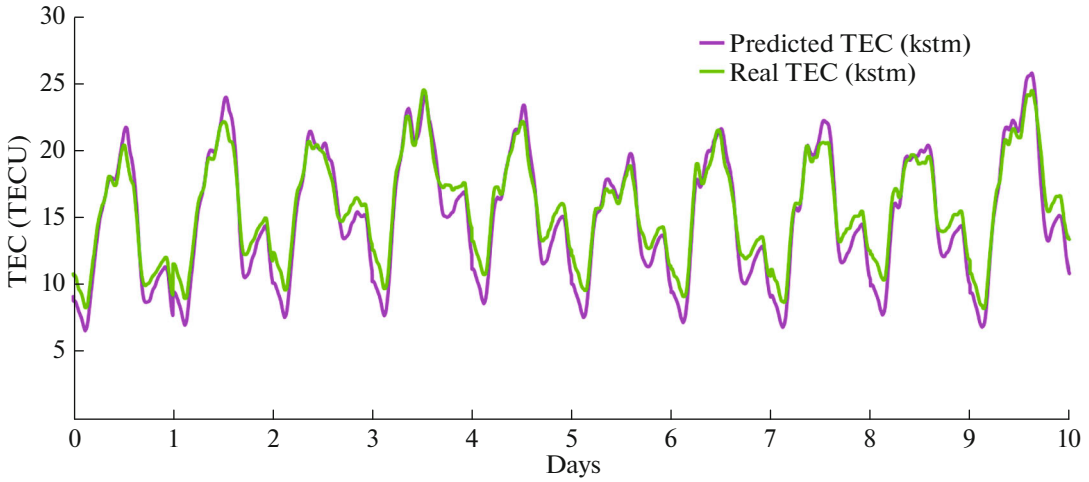

Fig. 6. 10-days distributions of spatio-predicted TEC and real TEC between October 02 and 11, 2010.

more successful than the techniques used in these studies. It can be said that ADF has a high performance for the spatio-temporal prediction. When the temporal and spatial predictions are compared with each other, it is observed that ADF is more successful tool in making temporal predictions according to the MSE values in Table 2.

The results presented in this section indicate that the ADF technique is a successful technique for the spatio-temporal prediction of Vertical Total Electron Content obtained from GPS receivers. The ADF algorithm can help to reduce the computational complexity for the prediction and be used to reconstruct GPS-TEC.

4. CONCLUSION

In this paper, an Adaptive Data Fusion technique is tested for the spatio-temporal prediction of GPS-

Table 2. Daily Mean Square Errors

Days	Mean Square Error (TECU)			
	spatial		temporal	
	May 02–11 2010	Oct. 02–11 2010	May 08–17 2011	Oct. 16–25 2011
1	3.1172	3.0261	3.1093	3.0938
2	3.1341	2.9988	2.4762	2.8182
3	2.9085	2.9497	3.3277	2.8850
4	3.1226	2.9005	2.9598	2.0396
5	3.0019	2.9404	3.1747	2.2410
6	2.9821	2.8392	2.6564	3.0174
7	3.0418	3.0412	2.3740	2.3597
8	3.5224	3.0390	2.9654	2.6479
9	3.2982	3.1746	2.5257	3.1345
10	3.4123	2.9735	2.5550	3.0949

TEC. This technique is used in two groups of application. In the first group of the application, the temporal-prediction is obtained using data of previous 10 days. The updating parameter μ is chosen 0.5 where the error $e_u(n,d)$ has the smallest value. The chosen year for the prediction is the solar maximum year. Although ionosphere is geomagnetically disturbed on May 2011, the ADF algorithm outputs the predictions in a small-error range. When the predicted-TEC and actual TEC data are compared with each other, it is observed that the characteristics of the predicted TEC and TEC are similar. Mean Square Errors (MSE) vary between 2 and 3.5 and it corresponds to less than 4 TECU.

In the second group of the application, six GPS receivers located corner regions and middle zone of Turkey are chosen for the spatial prediction. One receiver, namely kstm, is chosen as the central station to control and compare the predicted-TEC with actual TEC data. The window size M is 6 that equals to the number of the chosen stations. The updating parameter μ is also chosen 0.5 where the error $e_d(n,u)$ has the smallest value. It is observed that the predicted TEC has very close values to original TEC although MSEs in spatio-prediction are greater than those in the temporal-prediction. Chosen year is solar minimum year. There is no too much difference observed between the predicted TEC and the real TEC values. Characteristic distributions of the predict TEC and original TEC are similar with each other. Mean Square Errors (MSE) also vary between 2 and 3.5 in this group and it corresponds to less than 4 TECU.

When the Mean Square Error values are compared with the results in the literature, it is observed that ADF algorithm is more successful than the techniques used in the most studies in literature. It can be said that ADF has a high performance for the spatio-temporal prediction. When the temporal and spatial predictions are compared with each other, it is observed that ADF is more successful tool in making the temporal predictions according to the MSEs. It is expected that the ADF technique used in this study can be improved when the joint space-time analysis of ionospheric Total Electron Content is done over a denser GPS network in Turkey for the future works.

ACKNOWLEDGMENTS

The GIM-TEC, Satellite DCB and ephemeris data that are used in computation of IONOLAB-TEC are obtained from IGS Analysis Center of Jet Propulsion Laboratory (JPL) at (ftp://cddis.gsfc.nasa.gov/pub/gps/products/ionex). TNPGN-Active RINEX data set is made available to IONOLAB group for TUBITAK 109E055 project. This data set can be accessed by the permission from TUBITAK and General Command of Mapping of Turkish Army (http://www.hgk.msb.gov.tr/). The authors are grateful to anonymous Reviewers for their comments and contributions, which have been very helpful and constructive in improving the paper. Finally, the authors wish to thank IONOLAB group and Prof. Dr. Feza Arikan for personal communication on IONOLAB-TEC.

CONFLICT OF INTEREST

The authors declare that they have no conflict of interest.

REFERENCES

Afraimovich, E.L., Astafyeva, E.I., Demyanov, V.V., et al., A review of GPS/GLONASS studies of the ionospheric response to natural and anthropogenic processes and phenomena, *J. Space Weather Space Clim.*, 2013, vol. 3, no. A27, pp. 1–19.

Arikan, F., Erol, C.B., and Arikan, O., Regularized estimation of vertical total electron content from Global Positioning System data, *J. Geophys. Res.*, 2003, vol. 118, no. A12, pp. 1469–1480.

Arikan, F., Erol, C.B., and Arikan, O., Regularized estimation of vertical total electron content from GPS data for a desired time period, *Radio Sci.*, 2004, vol. 39, no. 6, pp. 1–10.

Arikan, F., Arikan, O., and Erol, C.B., Regularized estimation of TEC from GPS data for certain midlatitude stations and comparison with the IRI model, *Adv. Space Res.*, 2007, vol. 39, no. 5, pp. 867–874.

Arikan, F., Nayir, H., Sezen, U., and Arikan, O., Estimation of single station interfrequency receiver bias using GPS-TEC, *Radio Sci.*, 2008, vol. 43, no. 4, pp. 1–13.

Arikan, F., Arikan, O., Sezen, U., et al., Space–time interpolation and automatic mapping of TEC using TNP-GN-Active, *30th URSI General Assembly and Scientific Symposium*, IEEE, 2011.

Astafyeva, H. and Heki, K., Vertical TEC over seismically active region during low solar activity, *J. Atmos. Sol.-Terr. Phys.*, 2011, vol. 73, no. 13, pp. 1643–1652.

Benaskeur, A.R. and Rhéaume, F., Adaptive data fusion and sensor management for military applications, *Aerosp. Sci. Technol.*, 2007, vol. 11, pp. 327–338.

Brunini, C. and Azpilicueta, F., GPS slant total electron content accuracy using the single layer model under different geomagnetic regions and ionospheric conditions, *J. Geod.*, 2010, vol. 84, pp. 293–304.

Calais, E. and Minster, J.B., GPS detection of ionospheric perturbations following the January 17, 1994, Northridge Earthquake, *Geophys. Res. Lett.*, 1995, vol. 22, pp. 1045–1048.

Cander, Lj.R., Towards forecasting and mapping ionospheric space weather under cost actions, *Adv. Space Res.*, 2003, vol. 31, no. 4, pp. 957–964.

Deviren, M.N., Arikan, F., and Arikan, O., Spatio–temporal interpolation of total electron content using a GPS network, *Radio Sci.*, 2013, vol. 48, pp. 302–309.

Erken, F., Oksuztepe, E., and Kurum, H., Online adaptive decision fusion based torque ripple reduction in permanent magnet synchronous motor, *IET Electr. Power Appl.*, 2016, vol. 10, no. 3, pp. 189–196.

Erturk, O., Arikan, O., and Arikan, F., Tomographic reconstruction of the ionospheric electron density as a

function of space and time, *Adv. Space Res.*, 2009, vol. 43, no. 11, pp. 1702–1710.

García Rigo, A., Monte, E., Hernández Pajares, M., et al., Global prediction of the vertical total electron content of the ionosphere based on GPS data, *Radio Sci.*, 2011, vol. 46, pp. 1–13.

Gunay, O., Toreyin, B.U., Kose, K., and Cetin, A.E., Entropy-functional based online adaptive decision fusion framework with application to wildfire detection in video, *IEEE Trans. Image Process.*, 2012, vol. 21, no. 5, pp. 2853–2865.

Habarulema, J.B., Mckinnell, L.A., and Opperman, D.L., Regional GPS TEC modeling: Attempted spatial and temporal extrapolation of TEC using neural networks, *J. Geophys. Res.*, 2011, vol. 116, pp. 1–14.

Haykin, S. and Widrow, B., *Least-Mean-Square Adaptive Filters*, John Wiley & Sons, 2003.

Hofmann-Wellenhof, B., Lichtenegger, H., and Collins, J., *Global Positioning System: Theory and Practice*, Wien: Springer, 1992.

Hong, L., Adaptive data fusion, *Proceedings of IEEE International Conference on Systems, Man and Cybernetics*, IEEE, 1991.

Iijima, B.A., Harris, I.L., Ho, C.M., et al., Automated daily process for global ionospheric total electron content maps and satellite ocean altimeter ionospheric calibration based on Global Positioning System data, *J. Atmos. Sol.-Terr. Phys.*, 1999, vol. 61, pp. 1205–1218.

Karaman, Ö.A., Erken, F., and Cebeci, M., Decreasing harmonics via three phase parallel active power filter using online adaptive harmonic injection algorithm, *Teh. Vjesn.*, 2018, vol. 25, pp. 157–164.

Karatay, S., Arikan, F., and Arikan, O., Investigation of TEC variability due to seismic and geomagnetic disturbances in the ionosphere, *Radio Sci.*, 2010, vol. 45, pp. 1–12.

Karatay, S., Cinar, A., and Arikan, F., Ionospheric responses during equinox and solstice periods over Turkey, *Adv. Space Res.*, 2017, vol. 60, no. 9, pp. 1958–1967.

Kelly, M.C., *The Earth's Ionosphere Plasma Physics and Electrodynamics*, Academic, 2009.

Kim, B.-Ch. and Tinin, M.V., Effect of ionospheric irregularities on accuracy of dual-frequency GPS systems, *Geomagn. Aeron. (Engl. Transl.)*, 2007, vol. 47, no. 2, pp. 238–243.

Klein, A.L., *Sensor and Data Fusion Concepts and Applications*, SPIE Optical Engineering Press, 1993.

Kouris, S.S., Polimeris, K.V., and Cander, L.R., Specifications of TEC variability, *Adv. Space Res.*, 2005, vol. 37, no. 5, pp. 983–1004.

Llinas, J. and Singh, T., Adaptive data fusion processing: thoughts and perspectives, *Thirty-Second Asilomar Conference on Signals, Systems and Computers*, IEEE, 1998.

Liperovskya, V.A., Pokhotelov, O.A., Meister, C.V., and Liperovskaya, E.V., Physical models of coupling in the lithosphere–atmosphere–ionosphere system before earthquakes, *Geomagn. Aeron. (Engl. Transl.)*, 2008, vol. 48, no. 6, pp. 795–806.

Liu, J.Y., Chuo, Y.J., Shan, S.J., et al., Pre-earthquake ionospheric anomalies registered by continuous GPS TEC measurements, *Ann. Geophys.*, 2004, vol. 22, pp. 1585–1593.

Mannucci, A.J., Wilson, B.D., Yuan, D.N., et al., A global mapping technique for GPS-derived ionospheric total electron content measurements, *Radio Sci.*, 1998, vol. 33, no. 3, pp. 565–582.

McNamara, L.F., *Radio Amateurs Guide to the Ionosphere*, Krieger, 1994.

Nayir, H., Arikan, F., Arikan, O., and Erol, C.B., Total electron content estimation with Reg-Est, *J. Geophys. Res.*, 2007, vol. 112, no. A11, pp. 1–11.

Perevalova, N.P., Polyakova, A.S., and Zalizovski, A.V., Diurnal variations of the total electron content under quiet helio-geomagnetic conditions, *J. Atmos. Sol. Terr. Phys.*, 2010, vol. 72, pp. 997–1007.

Polekh, N.M., Pirog, O.M., Voeikov, S.V., et al., Ionospheric disturbances in the east-Asian region during the geomagnetic period in November 2004, *Geomagn. Aeron. (Engl. Transl.)*, 2006, vol. 46, no. 5, pp. 593–602.

Pulinets, S.A., Ouzunov, D., Ciraolo, L., et al., Thermal, atmospheric and ionospheric anomalies around the time of the Colima M7.8 earthquake of 21 January 2003, *Ann. Geophys.*, 2006, vol. 24, pp. 835–849.

Rishbeth, H., and Gariott, O.K., *Introduction to Ionospheric Physics*, Academic, 1969.

Seemala, G.K., *GPS-TEC Analysis Application*, Indian Institute of Geomagnetism, 2017.

Sezen, U., Arikan, F., Arikan, O., et al., Online automatic near-real time estimation of GPS-TEC: IONOLAB-TEC, *Space Weather*, 2013, vol. 11, no. 5, pp. 297–305.

Teunissen, P.J.G. and Odijk, D., Rank-defect integer estimation and phase-only modernized GPS ambiguity resolution, *J. Geod.*, 2003, vol. 76, nos. 9–10, pp. 523–535.

Troitsky, B.V., Ortikov, M.Y., Lobanov, K.A., et al., Ionospheric support of HF radiocommunication using maps of total electron content, *Geomagn. Aeron. (Engl. Transl.)*, 2007, vol. 47, no. 3, pp. 413–418.

Tulunay, E., Senalp, E.T., Cander, L.R., et al., Development of algorithms and software for forecasting, nowcasting and variability of TEC, *Ann. Geophys.*, 2004, vol. 47, nos. 2–3, pp. 1201–1214.

Tuna, H., Arikan, O., and Arikan, F., Regional model-based computerized ionospheric tomography using GPS measurements: IONOLAB-CIT, *Radio Sci.*, 2015, vol. 50, pp. 1062–1075.

Wu, S., Li, J., Zeng, X., and Bi, Y., Adaptive data fusion methods in information retrieval, *J. Assoc. Inf. Sci. Technol.*, 2014, vol. 65, no. 10, pp. 2048–2061.

Yasyukevich, Yu.Y., Mylnikova, A.A., and Polyakova, A.S., Estimating the total electron content absolute value from the GPS/GLONASS data, *Results Phys.*, 2015, vol. 5, pp. 32–33.

Zhukov, A., Sidorov, D., Mylnikova, A., and Yasyukevich, Y., Machine learning methodology for ionosphere total electron content nowcasting, *Int. J. Artif. Intell.*, 2018, vol. 16, no. 1, pp. 144–157.